International Journal of Applied Engineering Research
ISSN 0973-4562 Volume 10, Number 11 (2015) pp. 29893-29907

http://www.ripublication.com

Modelling and Analysis of Space Vector Modulation Based Three Phase Voltage Source Inverter

V.Indragandhi[#1], A. Kannabhiran[#2], R. Santhi[#3] and K. Giridharan[#4]
[#1, #2,#3]*Assistant Professor*, [#4]Professor,
Department of Electrical and Electronics Engineering,
SASTRA University, SRC Campus, Kumbakonam – 612001. India.
[#1]*arunindra08@gmail.com*, [#2]*mail2akannan@gmail.com*,
[#3]*shan_seee2k5@yahoo.co.in*, [#4]*giridharankam@gmail.com*,

Abstract

In this paper the space vector modulation based three phase voltage source inverter have been presented.In the proposed system modeling of space vectors , analysis and THD has calculated using the FFT analysis. In comparison with the THD of conventional system, the proposed system presents the lowest harmonic distortion. The speace vector based model have been compared with the carrier based model. A MATLAB/Simulink model of the proposed three phase inverter system was implemented . The validity of the proposed control schemes over a large operating range was verified through simulations.The operation in both grid connected and standalone power sytems has been discussed.

Keywords: Voltage source inverter,Space vector modulation,Total harmonic distorsion, PWM, Grid

Introduction

The developments in electronics and semiconductor technology have increased the potential of the power electronic systems. These high power devices are chiefly used to regulate and facilitate the flow of electric power, without compromising on the quality and meeting the stringent requirements imposed by the heavily loaded networks. Of these devices, these phase inverters are quite popular. The different circuit designs have been considerably explored by the researchers. The fundamental circuit of an inverter may apparently look simple, yet switching these devices accurately is a challenge. By eliminating unnecessary switching, Space vector Pulse Width Modulation (SVPWM) of the inverters provides output performance, a greater reliability, efficiency, and convenient digital realization, which is much superior to the inverters having conventional pulse width modulators. In a three-phase inverter,

Space Vector Pulse Width Modulation (SVPWM) additionally provides exceptional harmonic quality and higher under modulation range which increases the modulation factor from 78.5% (traditional) to 90.7% in sinusoidal PWM[1].Presently, three phase high and medium power applications mainly depends on the 3φ voltage source inverters. Four quadrant operation can be obtained in the Active-Reactive power plane. The applications of 3φ voltage source inverter include motor drive control, power factor improvement, distributed generation, standalone and grid connected systems, filtering, UPS and reactive power compensation. Usually, a series of rectangular periodic pulses are produced as the output of an inverter, having two special features: (1) Pulse adjacent to each other have different pulse widths and (2) the pulses are identical to the fundamental element of an inverter output. The industrial applications of the prominent modulation techniques are enumerated as follows: (1) Pulse width modulation (PWM) technique, including Sinusoidal PWM, Non sinusoidal, Random and Optimal; (2) Selected harmonic elimination; and (3) Hysteresis band current control.

Several papers have been published in the 1990s explaining the algorithms used in the SVM in the under-modulation range and implementation based on digital signal processor has explained[2-4] the overmodulation strategy for SVPWM of a three-stage inverter for neural network implementation.

In this paper, an overview of the three phase inverter based on the space vector modulation technique is discussed to familiarize its fundamental operation and modulation techniques. The actual implementation of the model is proposed with the help of MATLAB/Simulink model.

Three-Phase Voltage-Source Inverter

Static power converters mainly function as AC output waveform generators from a DC power supply. Depending on the type of AC output waveform, the voltage source inverters (VSIs) can be used to independently control the output voltage waveform[5] of the voltage source inverters, such as full bridge, half bridge, single phase, and three phase VSI, available, three phase VSI can be considered as remarkably distinguished due to it medium to high power applications[6]. The three phase VSIs requires a highly flexible algorithm in order to control inverter modulation. The modulation process involves applying fixed DC input voltage to the inverter to achieve a controlled AC output voltage. This process is completed by adjusting the ON and OFF periods of the inverter components, and referred to as pulse width modulation (PWM) control[7]. The application of SPWM techniques to inverters enables achievement of a sinusoidal output voltage with minimal undesired harmonics.

The three-phase (VSI) is designed with six power switches that allows bidirectional current flow. Two switches that are in same phase leg of the inverter operates in a complementary manner. At any given point, only one switch is permitted to be turned ON in the same leg, in order to protect the circuit from the DC link short circuit. The three-phase voltage-source inverter and the circuit topology of the bidirectional switch are presented in Figure 1.

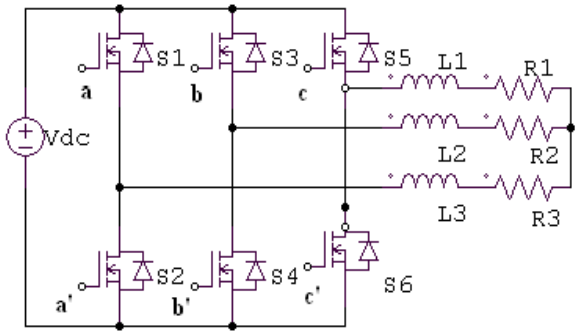

Figure 1: Circuit Topology For Three Phase VSI

In the three-phase full bridge inverter, six power MOSFET's are connected to a single DC power supply with no capacitor (Figure 1). This three phase inverter uses SVM, which is an algorithm for the control of pulse width modulation (PWM), to create AC waveforms. V_{an}, V_{bn} and V_{cn} are the output phase voltages from the inverter. PWM signals a, a', b, b', c, c' applied to the six power MOSFETs are controlled to regulate the output voltages. The six parallel diodes across the switches ensure free flow of current in both forward and reverse directions in A, B, C phase winding.

There are six switches in the inverters, referred to as S1, S2, S3, S4, S5, and S6. S1, S3 and S5 are the upper side switches, while S2, S4 and S6 and lower side switches. The state of the switches in the inverter legs are denoted as "1" and "-1" for the ON and OFF positions of a phase leg, respectively. It should be noted that in the switching level where the upper side switches S1, S3, S5 are ON, the lower-side switches S2, S4, and S6 are OFF, which is denoted by "1." On the contrary, when the switching level where the upper-side switches S1, S3, S5 are OFF, the lower-side switches S2, S4, S6 are ON and can be denoted by "-1". Because of the DC link capacitance, the DC voltage should not be interrupted and the distribution of the DC voltage into the three line to line voltages must not depend on the load. According to these switching rules, at any given time only one set of the upper and the lower switches must be kept closed all the time.

Distributed generation of energy uses emerging technologies that need an inverter to interface with the electrical distribution system. In order to benefit from this system, generation and associated loads should be considered as a micro-grid. When a disturbance occurs, the generation and associated loads can be separated from the distribution system to isolate the load of the micro-grid load from the disturbance without damaging the transmission grid's integrity, as well as continue service.

A micro-grid consists of distributed generation sources, controllable loads, and storage system that can function in grid connected mode or in isolated mode during disturbances. Microgrid increases the energy efficiency, decreases the overall energy consumption and enhances service quality and reliability of power supply[8,12]. Safety, stability, control and efficiency of the micro-grid are determined by the dynamic electrical characteristics of the multiple energy sources.

In the case of a stand-alone system, adequate storage ability is required by the system to handle the power deviation from the alternative energy sources used. As the

system has individual generation sources and loads, it can be regarded as a micro-grid. In the case of a grid-connected use, the other energy sources in the micro-grid can supply power both to the local loads and the utility grid. In addition to real power, these DG sources can also be used to give reactive power and voltage maintenance to the utility grid. The capacity of the storage device for these systems can be smaller if they are grid-connected since the grid can be used as system backup. However, when connected to a utility grid, significant operation and performance requirements, such as voltage, frequency and harmonic regulations, are imposed on the system.

Figure 2 demonstrates a typical output waveform of the three-phase full bridge inverter[11,13]. Three sinusoidal signals given in the figure have the same frequency with a phase difference of 120° from each other.

$$Va(t) = \sin \omega(t) \tag{1}$$

$$Va(t) = \sin(\omega(t) - 120) \tag{2}$$

$$Va(t) = \sin(\omega(t) + 120) \tag{3}$$

where $\omega_m = 2\pi f_m$, and f_m is the frequency of each sinusoidal signal.

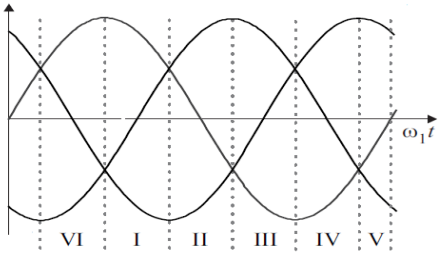

Figure 2: Three Phase Waveform

Modes of Operation

Figures 3 to 10 shows the various sector output voltages following the rules as given In all the operating modes, there is no conduction of same leg switches. The corresponding phase voltages are given below the respective figures.

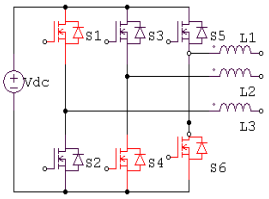

Figure 3: I (1,-1,-1)
$V_{an}= V_{dc}/2$ $V_{bn}=V_{cn}=-V_{dc}/2$

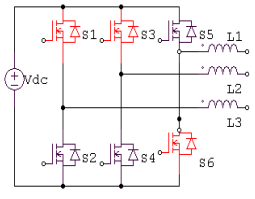

Figure 4: II(1,1,-1)
$V_{an}= V_{bn}= V_{dc}/2$ $V_{cn}=-V_{dc}/2$

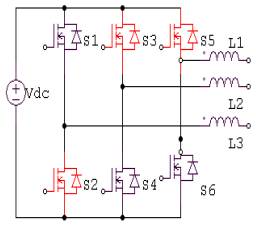

Figure 5: III (-1, 1, 1)
V_{an}= -V_{dc}/2 V_{bn}=V_{cn}=V_{dc}/2

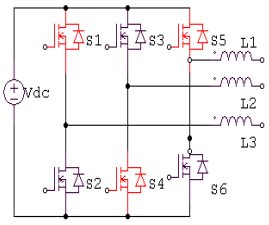

Figure 6: IV (1,-1, 1)
V_{bn}= -V_{dc}/2 V_{an}=V_{cn}=V_{dc}/2

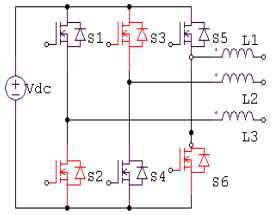

Figure 7: V (-1, 1,-1)
V_{bn}= V_{dc}/2 V_{an}=V_{cn}=-V_{dc}/2

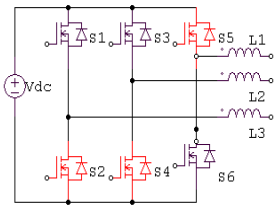

Figure 8: VI (-1,-1, 1)
V_{an}=V_{bn}= -V_{dc}/2 V_{cn}=V_{dc}/2

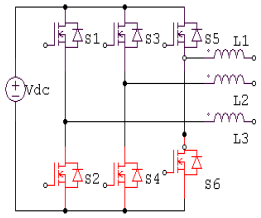

Figure 9:VII (-1,-1,-1)
V_{bn}= V_{an}=V_{cn}=-V_{dc}/2

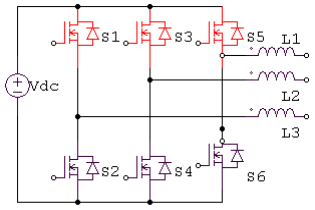

Figure 10: VIII (1, 1, 1)
V_{bn}= V_{an}=V_{cn}=V_{dc}/2

By choosing the modulation and carrier signals appropriately, space-vector modulation strategy can be attained. All the modulation by means carrier approach can be realized in the space vector hexagon by finding the exact voltage space vector order.

Table 1: Switching States and Output Voltages

Space Vector Voltage	**Switches**		**Output Voltages**		
	ON	**OFF**	**V_{an}**	**V_{bn}**	**V_{cn}**
-1-1-1	S2,S4,S6	S1,S3,S5	-Vdc/2	-Vdc/2	-Vdc/2
V1(-1-11)	S2,S4,S5	S1,S3,S6	-Vdc/2	-Vdc/2	Vdc/2
V2(-11-1)	S2,S3,S6	S1,S4,S5	-Vdc/2	Vdc/2	-Vdc/2
V3(-111)	S2,S3,S5	S1,S4,S6	-Vdc/2	Vdc/2	Vdc/2
V4(1-11)	S1,S4,S5	S2,S3,S6	Vdc/2	-Vdc/2	Vdc/2
V5(1-1-1)	S1,S4,S6	S2,S3,S5	Vdc/2	-Vdc/2	-Vdc/2
V6(11-1)	S1,S3,S6	S2,S4,S5	Vdc/2	Vdc/2	-Vdc/2
111	S1,S3,S5	S2,S4,S6	Vdc/2	Vdc/2	Vdc/2

The length of the V1, V2, … V8 depends on the time taken on each state, which is derived by the following equations. Switching periods are denoted by *T*'s and the radius of the hexagons are denoted by $2/3V_{dc}$.

$$V_1 = \frac{2}{3}\frac{T1}{Ts}V_{dc} \tag{4}$$

$$V_2 = \frac{2}{3}\frac{T2}{Ts}V_{dc} \tag{5}$$

$$V_3 = \frac{2}{3}\frac{T3}{Ts}V_{dc} \tag{6}$$

$$V_4 = \frac{2}{3}\frac{T4}{Ts}V_{dc} \tag{7}$$

$$V_5 = \frac{2}{3}\frac{T5}{Ts}V_{dc} \tag{8}$$

$$V_6 = \frac{2}{3}\frac{T6}{Ts}V_{dc} \tag{9}$$

By applying sine laws, the time period for each sector can be calculated as follows:

$$\frac{2V_o}{\sqrt{3}} = \frac{V_2}{\sin\theta} \tag{10}$$

$$\frac{2V_o}{\sqrt{3}} = \frac{V_2}{\sin(60-\theta)} \tag{11}$$

$$\frac{2V_o}{\sqrt{3}} = \frac{\frac{T_2}{Ts}*\frac{2}{3}V_{dc}}{\sin(60-\theta)} \tag{12}$$

$$\frac{2V_o}{\sqrt{3}} = \frac{\frac{T_1}{Ts}*\frac{2}{3}V_{dc}}{\sin\theta} \tag{13}$$

The time taken for section I and section II are estimated through the following equations:

$$\frac{\sqrt{3}T_S\sin\theta V_O}{V_{dc}} = T_1 \tag{14}$$

$$\frac{\sqrt{3}T_S\sin(60-\theta)V_o}{V_{dc}} = T_2 \tag{15}$$

Figure 11 shows the sectors I to VI with corresponding voltages as stationary vectors in the plane. The abc parameters are converted into αβ transformation through the length of the vectors and the DC-link voltage, which are calculated, along with their angular position in the plane.

The boundaries of the space vector voltage will form a regular hexagon, which determines the limits between the linear modulation and overmodulation section. To maintain balanced sinusoidal line-to-line converter voltages, the reference voltage

vector should follow a circular trajectory. Any operation that occurs outside of the hexagon results in over modulation.

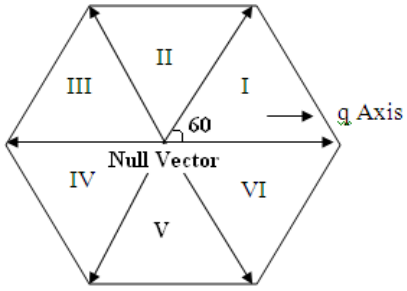

Figure 11: Space Vector Hexagon

Table 2 depicts the vector V2 (-1, 1, -1) that produces the converter voltages.

Table 2: Space Vector Displacement and Angle

Space vector voltage	**Angle in degree**	**Length**
V1(1,-1,-1)	0	0.67
V2(1,1,-1)	60	0.67
V3(-1,1,-1)	120	0.67
V4(-1,1,1)	180	0.67
V5(-1,-1,1)	240	0.67
V6(1,-1,1)	300	0.67

The transformation of is applied in the αβ plane to obtain αβ and the components of V2.

$$\begin{bmatrix} V_\alpha \\ V_\beta \\ V_0 \end{bmatrix} = \frac{2}{3V_{dc}} \begin{bmatrix} 1 & 1/2 & -1/2 \\ 0 & \sqrt{3}/2 & -\sqrt{3}/2 \\ 1/\sqrt{2} & 1/\sqrt{2} & 1/\sqrt{2} \end{bmatrix} * \begin{bmatrix} V_a \\ V_b \\ V_c \end{bmatrix} \quad (16)$$

V2 (-1 1 -1)

$$\begin{bmatrix} V_{2\alpha} \\ V_{2\beta} \end{bmatrix} = \frac{2}{3V_{dc}} \begin{bmatrix} 1 & 1/2 & -1/2 \\ 0 & \sqrt{3}/2 & -\sqrt{3}/2 \end{bmatrix} * \begin{bmatrix} V_{a1} \\ V_{a2} \\ V_{a3} \end{bmatrix} \quad (17)$$

$$\begin{bmatrix} V_{2\alpha} \\ V_{2\beta} \end{bmatrix} = \frac{2}{3V_{dc}} \begin{bmatrix} 1 & 1/2 & -1/2 \\ 0 & \sqrt{3}/2 & -\sqrt{3}/2 \end{bmatrix} * \begin{bmatrix} -V_{dc}/2 \\ V_{dc}/2 \\ -V_{dc}/2 \end{bmatrix} \quad (18)$$

$$V_{2\alpha} = \frac{2}{3V_{dc}} \left[-\frac{V_{dc}}{2} + \frac{V_{dc}}{4} + \frac{V_{dc}}{4} \right] \quad (19)$$

$$V_{2\alpha} = \frac{2}{3V_{dc}} \left[-\frac{V_{dc}}{2}\right] \tag{20}$$

$$V_{2\alpha} = -\frac{1}{3} \tag{21}$$

$$V_{2\beta} = \frac{2}{3V_{dc}} \left[0 + \frac{\sqrt{3}V_{dc}}{4} + \frac{\sqrt{3}V_{dc}}{4}\right] \tag{22}$$

$$V_{2\alpha} = \frac{2}{3V_{dc}} \left[\frac{2\sqrt{3}V_{dc}}{4}\right] \tag{23}$$

$$V_{2\alpha} = \frac{1}{\sqrt{3}} \tag{24}$$

$$V_{2\beta} = \frac{2}{3V_{dc}} \left[0 + \frac{\sqrt{3}V_{dc}}{4} + \frac{\sqrt{3}V_{dc}}{4}\right] \tag{25}$$

$$V_{2\beta} = \frac{2}{3V_{dc}} \left[\frac{2\sqrt{3}V_{dc}}{4}\right] \tag{26}$$

$$V_{2\beta} = \frac{1}{\sqrt{3}} \tag{27}$$

The length between space vector voltages, which is equal to 2/3 are determined using the following equations:

$$|V| = \sqrt{(1/3)^2 + (1/\sqrt{3})^2} \tag{28}$$

$$|V| = 2/3 \tag{29}$$

The angle between space vector voltage and the reference q axis, which is equal to 60 are determined as follows:

$$\angle V = \tan^{-1} \frac{1/\sqrt{3}}{1/3} \tag{30}$$

$$\angle V = 60 \tag{31}$$

The three phase sine wave output voltage with variable frequency and constant amplitude is given to the three phase abc parameter through two phase αβ parameter transformation block. The three phase input signals are 120° out of phase with each other. The αβ vector is used to find the sector of αβ plane at which the output voltage vector lies. All αβ plane consists of six sectors with 60° displacement. The ramp generator generates the time taken for the switching sequence, and the timing for voltage vector is estimated by the switching time calculator. The sector in which the voltage vector is present is taken as the input for the timing calculator. The gate logic generator compares the timing sequence from ramp generator and gate timing signals. Based on the error, it activates the power switches present in the inverter at the proper time. (figure12)

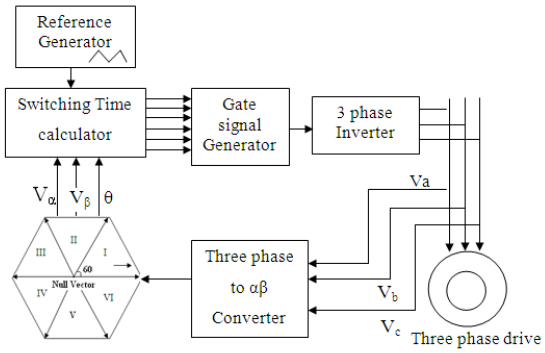

Figure 12: Control block for three phase VSI

Simulation Results and Discussion

The conduction of switches with switching time periods in the second sector are shown in Figure 13. At voltage V0 all the switches are in OFF condition, at V7 all the switches are in ON condition.

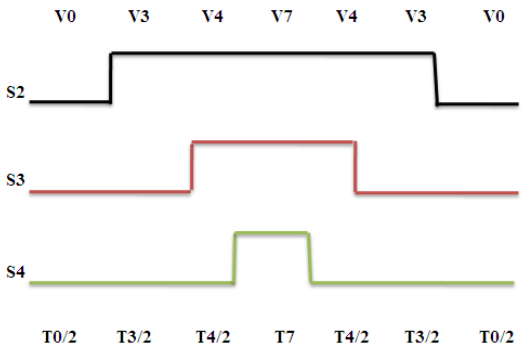

Figure 13: Switching Pattern

The total switching time period is the difference between (T_0+T_7) and corresponding sector switches conduction period. The total switching period for all the sectors are calculated as per the formula given in Table 3.

Table 3: Total Switching Time In Each Sector

Sector I	$T_S=T_0+T_7-(T_1+T_2)$
Sector II	$T_S=T_0+T_7-(T_2+T_3)$
Sector III	$T_S=T_0+T_7-(T_3+T_4)$
Sector IV	$T_S=T_0+T_7-(T_4+T_5)$
Sector V	$T_S=T_0+T_7-(T_5+T_6)$
Sector VI	$T_S=T_0+T_7-(T_6+T_1)$

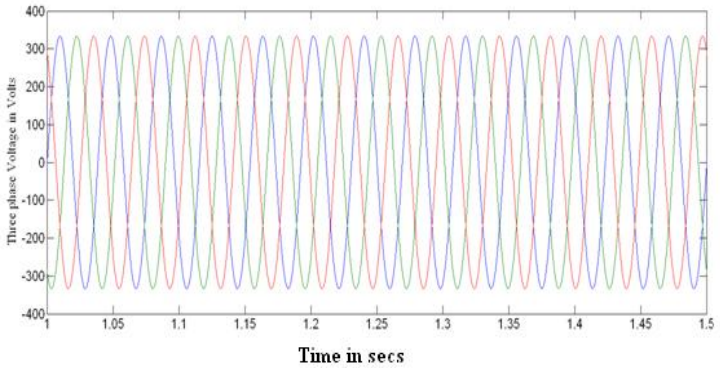

Figure 14: Three-phase inverter output voltage

The output voltage and output current of the grid connected system are shown in Figure 14-15. The current Total Harmonic Distortion (THD) for the proposed system was calculated for five cycles. The FFT analysis conducted during the simulation was found to be about 6.60% for fundamental frequency of 50Hz. In comparison with the THD of conventional system, the THD obtained from proposed system was less. In this experiment, the THD was calculated up to 300 Hz for capturing the fundamental frequency spectrum as shown in Figure 16.

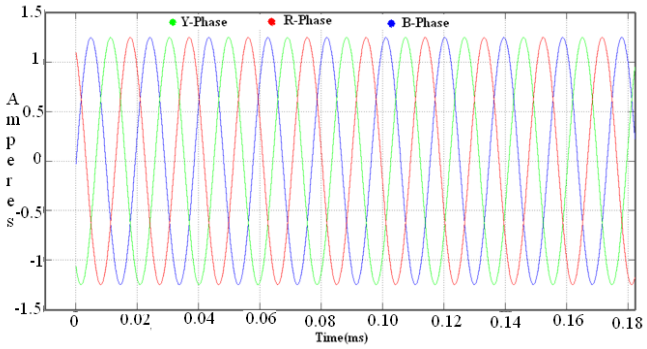

Figure 15: Three-Phase Inverter Output Current

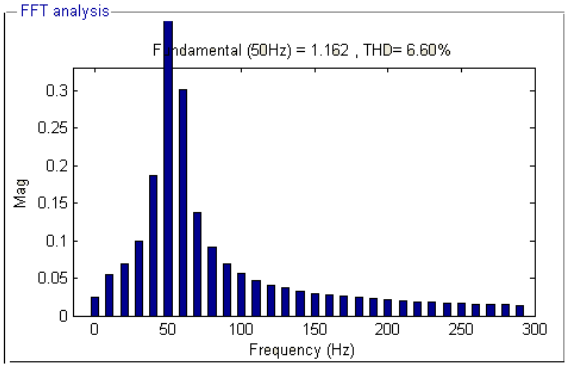

Figure 16: THD of The Proposed System

Based on the FFT results, the TDH calculated using the below give formula was found to be up to 300Hz:

$$THD_f = \sqrt{\sum_2^n f_n^2 / f_1} \quad (32)$$

Where *f* stands for phase current or phase voltage, f_n represents the *n*-th component in the harmonic spectrum close to 300 Hz frequency. The AC output voltage harmonic contents are shown in Table 5.5. The even harmonics that are present in the output cancelled out each other. By the use of filter, the few higher order harmonics that interfere are filtered out.

Sampling time = $5*10^{-5}$ Seconds
Samples per second = 400
DC component = 11.3
Fundamental = 224 rms
Total Harmonic Distortion = 3.85%

Table 5: Voltage THD

Frequency (Hertz)	Harmonics (%)	Order of harmonics
0	3.57	DC
50	100	Fundamental
100	3.21	2nd order
150	1.40	3rd order
200	0.88	4th order
250	0.64	5th order
300	0.51	6th order
350	0.42	7th order
400	0.36	8th order
450	0.31	9th order
500	0.28	10th order
550	0.25	11th order
600	0.23	12th order
650	0.21	13th order
700	0.19	14th order
750	0.18	15th order
800	0.17	16th order
850	0.16	17th order
900	0.15	18th order
950	0.14	19th order

A MATLAB/Simulink model of the proposed three phase inverter system was implemented using the SimPowerSystems block-set. The validity of the proposed control schemes over a large operating range was verified through simulations. Figure

17 shows the SIMULINK model for generation timing signals to SVM based three phase inverter.

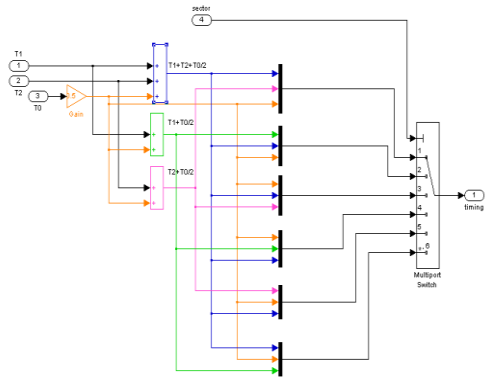

Figure 17: Generation Block For Timing Signals

Figure 18 shows the SIMULINK model for generation pulses based on the timing received from the last block to SVM based three phase inverter.

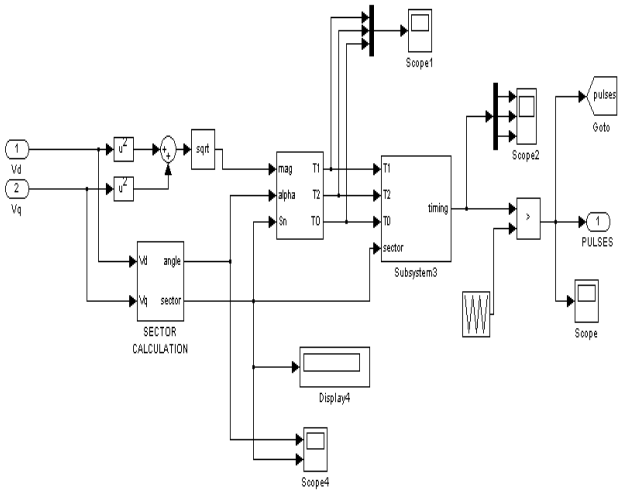

Figure 18: Generation Block For Pulses

Figure 19 shows T0 ,T1 and T2 signals obtained in the Scope1.

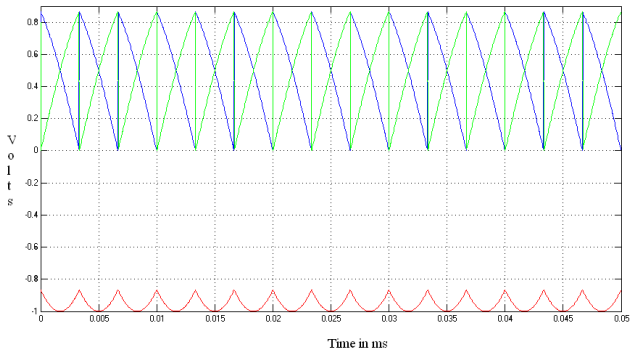

Figure 19: T0, T1 And T2 Signals Waveform

Figure 20 shows the timing signals obtained from Scope 2 as being interwoven with the reference sawtooth waveform.

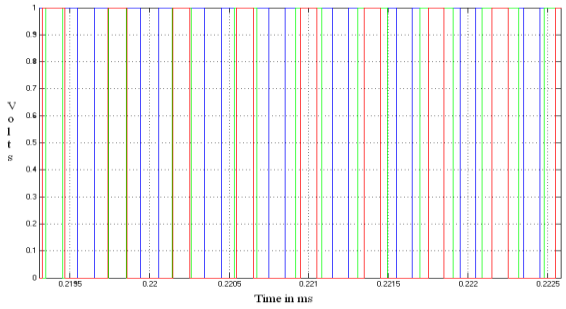

Figure 20: The Timing Signals Waveform

The pulse generated in the three phase inverter after the switches were turned ON is shown in Figure 21. The figure illustrates the mixing of the pulse with the reference sawtooth waveform obtained in Scope 3.

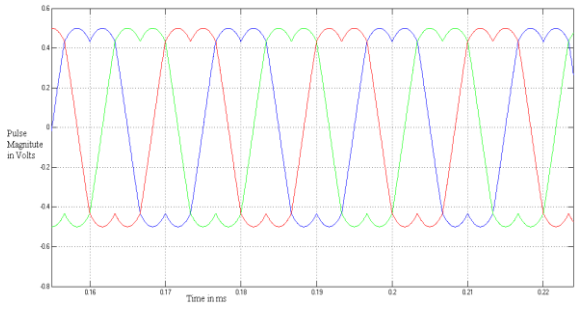

Figure 21: Generated Pulses

Figure 22 shows the SIMULINK model of entire space vector modulation based three phase inverter.

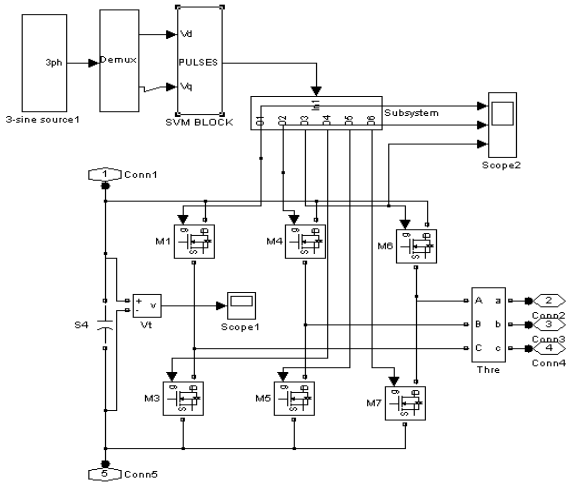

Figure 22: Model For Space Vector Modulation Based Three Phase Inverter

Conclusion

In this paper discussed the three phase voltage source inverter that can independently control the ouput voltage waveform. A method to generate pulse width modulation signals for control of six switch three-phase inverters has been presented.In the proposed system, THD was calculated for five cycles. The FFT analysis conducted during the simulation was found to be about 6.60% for fundamental frequency of 50Hz. In comparison with the THD of conventional system, the proposed system presents the lowest harmonic distortion. A MATLAB/Simulink model of the proposed three phase inverter system was implemented . The validity of the proposed control schemes over a large operating range was verified through simulations.

References

[1] S.K. Monndal, J.O.P Pinto and B.K. Bose " A neural network based space vector PWM controller for a three level voltage fed inverted induction motor drive" IEEE Trans. Ind. Applicat. 38, pp. 660-669, 2002.

[2] J. Zhang, "High performance control of a three-level IGBT inverter fed ac drive" Proceedings IEEE IECON Conf. pp. 22-28, 1995.

[3] M. Koyama, T. Fujii, R. Uchida and T. Kawabata,, "Space vector based new PWM method for large capacity three-level GTO inverter" Proceedings IEEE IECON Conf. pp. 271-276, 1992.

[4] H. L. Liu, N..S. Choi an G.H. Cho. "DSP based space vector pulse width modulation for three-level inverter with dc-link voltage balancing" Proceedings IEEE IECON Conf. pp. 197-203, 1991.

[5] Gupta A. & Kumar S., "Analysis of three phase space vector pwm voltage source inverter for ASD's" International Journal of Emerging Technology and Advanced Engineering, 2(10) 163-168, 2012.

[6] Holtz J., "Pulse width modulation for electronic power conversion" Proceedings IEEE, 82 1194-1214, 1994.
[7] M. H. Rashid, Ed., Power Electronics Handbook. San Diego, CA: Academic, 2001.
[8] A. Oudalov and A. Fidigatti, "Adaptive network protection in microgrids" International Journal of Distributed Energy Source, 4, pp. 201–205,2009.
[9] S. A. Saleh, C. R. Moloney, and M. Azizur Rahman, "Analysis and Development of Wavelet Modulation for Three-Phase Voltage-Source Inverters" IEEE Transactions On Industrial Electronics, 58 (8), 2011.
[10] Stephanie Katherine Teixeira Miller, 2008"Analysis of three-phase rectifiers with ac-side switches and interleaved three-phase voltage-source converters" Degree of Doctor of Philosophy November, 2008.
[11] Giovanna Oriti and Alexander L. Julian, "Three-phase VSI with FPGA-based multisampled space vector modulation" IEEE Transactions On Industry Applications, 47(4), 2011.
[12] N. Mohan, T. M. Undeland, and W. P. Robbins, "Power Electronics: Converters, Applications, and Design". New York: Wiley, 1995.
[13] Subrata K. Modal, "Space vector pulse width modulation of three-level inverter extending operation into overmodulation region" IEEE, 18(2), 604-611, 2003.